

International Council for
the Exploration of the Sea

ICES CM 2001/ Q: 09
Theme Session on Catchability and Abundance Indicators
-the Influence of Environment and Fish Behaviour (Session: Q)

Modelling herring target strength pressure dependence in the frequency domain

By

Natalia Gorska¹ and Egil Ona²

¹Institute of Oceanology of Polish Academy of Sciences,
ul. Powstancow Warszawy 55, PL-81 - 712 Sopot, Poland

tel.: +48 58551 72 81,

fax: +48 58 551 2130,

email: gorska@iopan.gda.pl

²Institute of Marine Research, P.O.Box 1870, Nordnes, N-5817 Bergen, Norway

tel.: +47 55 23 85 00,

fax +47 55 23 85 84,

email: egil.ona@imr.no

ABSTRACT

Improved understanding of the acoustic scattering properties of the fish is needed when trying to remove potential bias in acoustic abundance estimates. The paper addresses the problem of systematic pressure or depth dependency in herring target strength, as due to the uncompensated compression of the swimbladder with depth. As a first stage, a theoretical approach to the problem is developed using a Modal-Based Deformed Cylinder Model. This includes the pressure effects on the swimbladder and the effect of the fish flesh. Using the theoretical solutions obtained, a sensitivity analysis on fish target strength with pressure is made at various acoustic frequencies, and compared with real target strength data on adult herring.

INTRODUCTION

The target strength is a primary factor in acoustic abundance estimates of fish. Among many factors that may affect the target strength, changes related to the swimbladder are recognised as the most important.

Herring belongs to physostomatous fish. All morphological investigations and experiments with live herring (Blaxter & Batty, 1984, Brawn, 1962, Fahlen, 1967, Ona, 1990) confirmed the lack of gas production in herring swimbladder. Under external pressure variability, the volume of herring swimbladder will therefore change. Ona (1990) demonstrated that the volume reduces with pressure increasing according to Boyle's law. As herring often conducts extensive vertical migration over a 40 atmospheres pressure range, only 1/41 of swimbladder surface volume should remain at 400 m depth. As the swimbladder

acts as the main acoustic reflector in the fish, such changes should drastically influence its acoustic backscattering properties.

The depth dependence of Norwegian Spring Spawning herring target strength has been confirmed by measurements made from R/V “Fjordfangst” on a deep moored aquaculture plant at Tysnes, south of Austevoll (Ona *et al.*, 2001a) in April 1997. A large 4500 m³ cage, within which the herring could swim freely, was then used. A 38 kHz, pressure stabilised, submersible split-beam transducer was here used to measure the target strength of the caged herring over a depth range from 0 to 100 m.

The trial was conducted in order to explain the observed target strength depth dependence *in situ*, which was analysed using the full free compression model (Ona *et al.*, 2001a). However, the model gave a significantly slower depth reduction in herring target strength than it was observed in the measurements. Most likely, the discrepancy can be explained by the limitations of the model. The model accounts only for the backscattering by the swimbladder and does not consider acoustic contribution from the fish flesh, which may become exceedingly important as the swimbladder contracts. Moreover, the shrinkage rates of the swimbladder individual dimensions, which influence on the target strength depth dependence, are assumed to be identical. However, some experimental studies {Blaxter, 1979, Ona, 1990) of actual shrinkage rates indicate that the contraction is not iso-metric, mainly due to the attachment of the bladder wall to the surrounding tissue. In summary, it was therefore reasonable to develop a model which also considered the fish flesh contribution to the backscattering cross section, as well as facilitating a sensitivity analysis of herring target strength with varying reduction rates of the swimbladder individual dimensions.

In this paper we propose the model enabling all these studies. This is the Modal Based Deformed Cylinder Model (MB-DCM), developed by Stanton (1988, 1989), in which we introduce swimbladder depth compression. The main solutions for herring backscattering cross section are presented in the paper. The analyses of herring target strength depth dependency were made at several discrete frequencies, often used during herring surveys. The influence of the backscattering by the fish body and the importance of increased knowledge of how herring swimbladder actually contracts with depth, are demonstrated. The analysis is at this stage done for the broadside incidence case only, in which herring are oriented normally or near normally to the sound incidence direction. The comparison with the measurement data is therefore done on selected maximum target strength data only.

MAIN EQUATIONS

In this section the analytical solutions for backscattering cross section of fish are presented.

According to (Medwin & Clay, 1998), the backscattering amplitude of the whole fish, f_{tot} is the coherent sum of the backscattering amplitudes from the fish body, f_b , and swimbladder, $f_{sb}(z)$. Accounting for the depth compression of swimbladder of a typical herring, we should introduce the depth dependence of the swimbladder backscattering amplitude in the solution:

$$f_{tot}(z) = f_{sb}(z) + f_b \quad (1)$$

According to the definition, the differential backscattering cross section of whole fish and its target strength can be expressed as:

$$\sigma_{tot}(z) = |f_{sb}(z) + f_b|^2 \quad (2)$$

$$TS(z) = 10 \log \sigma_{tot}(z) \quad (3)$$

respectively.

To obtain the analytical solution for the backscattering amplitudes the geometrical shape of the swimbladder and fish body should be taken into account. Following the papers (Furusawa, 1988, Ye & Furusawa, 1995, Ye, 1996, Ye & Farmer 1996) we approximate them respectively by a gas-filled and a fluid-like prolate spheroids.

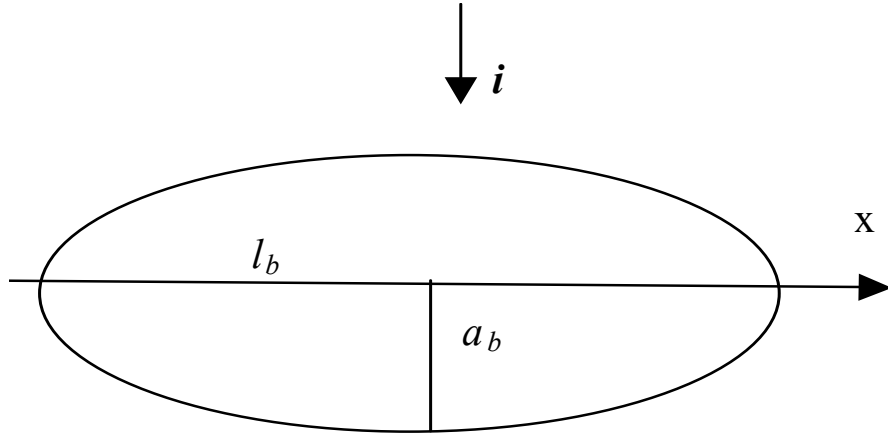


Fig. 1
Prolate spheroid geometry of fish body.

The changes of the semi-minor axis lengths $a_{sb}(x,z)$ and $a_b(x)$ along the major axis of the prolate spheroid (x is the co-ordinate along the major axis, see Fig. 1) are described by

$$a_{sb}(x,z) = a_0^{sb}(z) \left[1 - (x/(l_{sb}(z)/2))^2 \right]^{1/2} \quad (4)$$

and

$$a_b(x) = a_0^b \left[1 - (x/(l_b/2))^2 \right]^{1/2} \quad (5)$$

where the functions $l_{sb}(z)$ and $a_0^{sb}(z)$ describe the depth dependence of the major and semi-minor axes of the prolate spheroidal swimbladder caused by swimbladder compression. The parameter l_b denotes the body major axis length.

The acoustic properties of the fish swimbladder and flesh are described by the sound speed and density contrasts, h_{sb} g_{sb} , and, h_b g_b , respectively: $h_{sb} = c_{sb}/c_1$, $g_{sb} = \rho_{sb}/\rho_1$, and $h_b = c_b/c_1$, $g_b = \rho_b/\rho_1$. Here and further the subscripts „sb” and „b” refer to the properties inside the swimbladder and fish flesh respectively. The parameters ρ_1 and c_1 are the density and sound speed in the surrounding water.

We introduce into the Modal Based Deformed Cylinder Model (Stanton, 1988, 1989) the depth dependence of swimbladder dimensions. Backscattering amplitudes of swimbladder and fish can be written respectively as:

$$f_0^{sb}(z) = - \frac{i}{\pi} l_{sb}(z) \int_0^1 du \sum_{m=0}^{\infty} b_m^{sb}(z,u). \quad (6)$$

$$f_0^b = - \frac{i}{\pi} l_b \int_0^1 du \sum_{m=0}^{\infty} b_m^b(u). \quad (7)$$

where the integration over the u – variable means the integration over the main axis of swimbladder and fish body. Here $u=x/(l_{sb}(z)/2)$ and $du=dx/(l_{sb}(z)/2)$ in the first integral (Eq. (6)) and $u=x/(l_b/2)$ and $du=dx/(l_b/2)$ in the second integral (Eq. (6)).

The coefficients $b_m^{sb}(z)$ and b_m^b can be expressed as:

$$b_m^{sb}(z) = \frac{\varepsilon_m (-1)^m}{1 + iC_m^{sb}(z)} \quad (8)$$

$$b_m^b = \frac{\varepsilon_m (-1)^m}{1 + iC_m^b} \quad (9)$$

The Neumann factor $\varepsilon_m = 1$ for $m=0$, and $\varepsilon_m = 2$ for $m>0$. For the coefficients $C_m^{sb}(z)$ and C_m^b we use the expressions, presented in (Stanton, 1988), Eq. (12) from the quoted paper, introducing the depth dependence of the swimbladder radius a_{sb} . The coefficients represent the complicated non-linear combination of the Neumann and Bessel functions and their derivatives. C_m^b and $C_m^{sb}(z)$ depend on the contrasts of fish flesh and swimbladder and on the dimensionless parameters ka_0^b and $ka_0^{sb}(z)$ respectively. Here $k = 2\pi f / c_1$ is the wave number in seawater, f is the acoustic frequency.

The depth dependence of the semi-minor and major axes of the compressed swimbladder is required to solve the problem. Unfortunately, the question – how the individual herring swimbladder dimensions contract with depth – has not been replied yet. Nonnumerous studies give only a preliminary answer (Blaxter, 1979, Ona, 1990). Therefore, to define the dependencies $a_0^{sb}(z)$ and $l_{sb}(z)$ we can use the only checked founding that the volume of herring swimbladder $V(z)$ is compressed with depth, according to Boyle's law (Ona, 1990) and can be expressed by: $V(z) = V_0(1 + z/10)^{-1}$, where V_0 is the volume at the surface. Using this founding, we assume that semi-minor and major lengths decrease during the compression by the following manner:

$$a_0^{sb}(z) = a_{sb}(0) (1 + z/10)^{-\alpha} \quad (10)$$

$$l_{sb}(z) = l_{sb}(0) (1 + z/10)^{-\beta} \quad (11)$$

where α and β are the contraction factors for the corresponding dimensions. Boyle's law requires that $2\alpha + \beta = 1$.

We consider in our paper only the broadside incidence case (the herring orientation is near normal to the incident sound).

NUMERICAL RESULTS

The results of numerical study of the depth dependence of the backscattering cross sections of swimbladder (top plot) and whole fish (bottom plot) are summarised in Fig. 2 a, b.

Various curves in each plot refer to four acoustic frequencies, which are frequently used in herring abundance estimation - 18 kHz (square-marked curve), 38 kHz (diamonds), 120 kHz (triangles) and 200 kHz (circles). The nondifferential backscattering cross section in cm^2 is presented in horizontal axis.

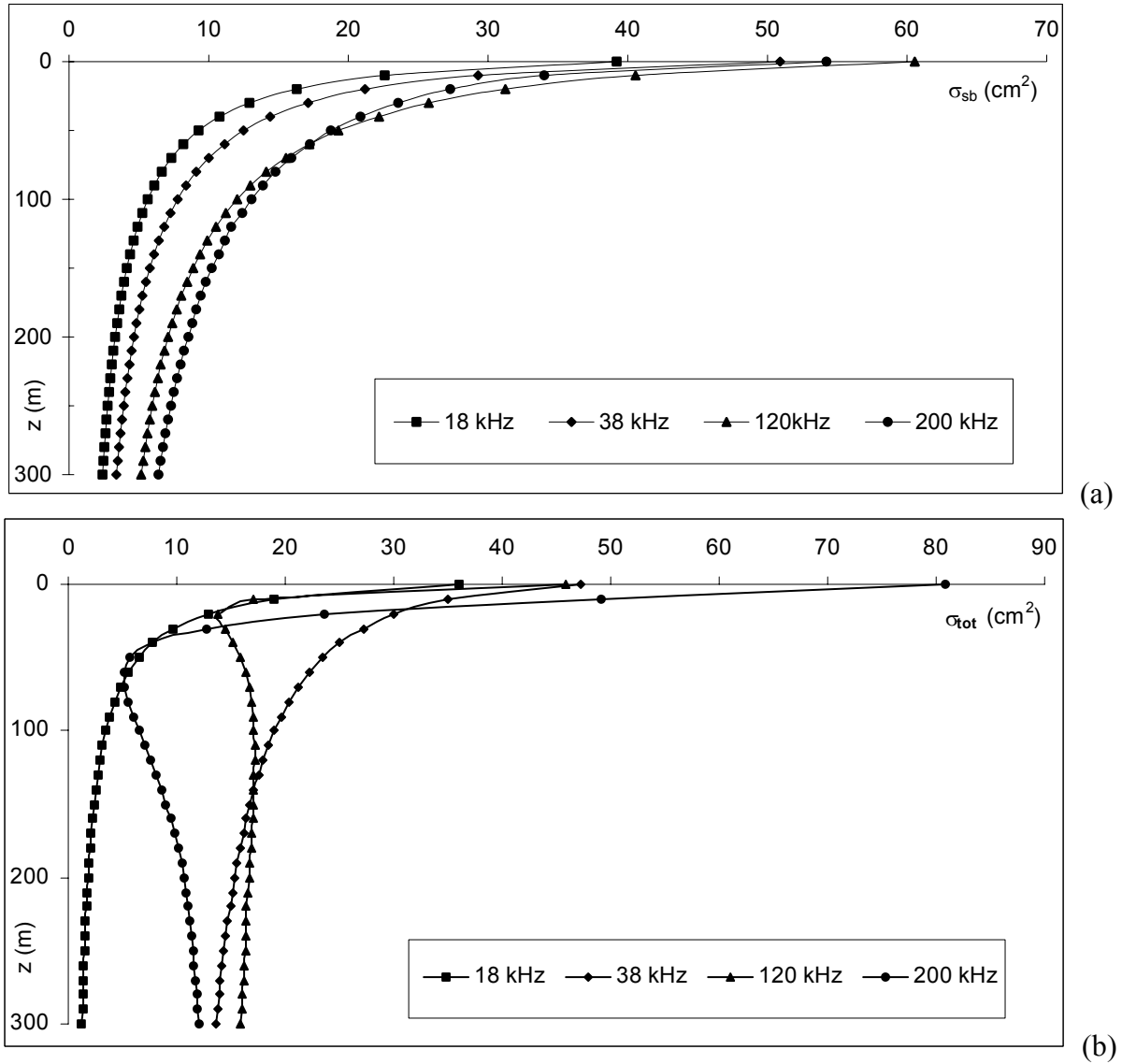


Fig. 2

Depth dependence of the backscattering cross section of swimbladder (a) and whole fish (b).

Here $\sigma_{sw}(z) = |f_{sw}(z)|^2$ describes the swimbladder backscattering cross section. The computations are performed for a herring with total length 32 cm, the ratio of the swimbladder length to the total length 0.26, the dorsal width of swimbladder and fish body 1 cm and 2 cm respectively and for the spatial displacement between swimbladder and fish body 2 cm. The density and sound speed contrasts used are (1.04; 1.04) and (0.00129; 0.23) for fish flesh and fish swimbladder respectively. The contraction factors α and β are equal to 1/3.

Over the entire frequency range a monotonically decreasing swimbladder backscattering cross section is observed. For the whole fish backscattering cross section the monotonic decreasing is observed only at 18 and 38 kHz (square- and diamond- marked

curves). At higher frequencies (120 and 200 kHz) the dependence is more complicated and does not repeat the monotonic nature, as for the swimbladder. The lack of similarity indicates that the fish flesh contribution has become significant.

To understand how the frequency dependence changes with depth the calculations, result of which are shown in Fig. 3, have been made. The calculation parameters are the same as for Fig. 2. The ratio of whole fish backscattering cross section at different frequencies to the backscattering cross section at 38 kHz is presented on the horizontal axis. We can see that the frequency dependence varies with depth by the following manner. Near the surface the backscattering cross section is the largest at 200 kHz. In the layers deeper than 140 m the largest backscattering cross section is observed at 120 kHz and the smallest at 18 kHz.

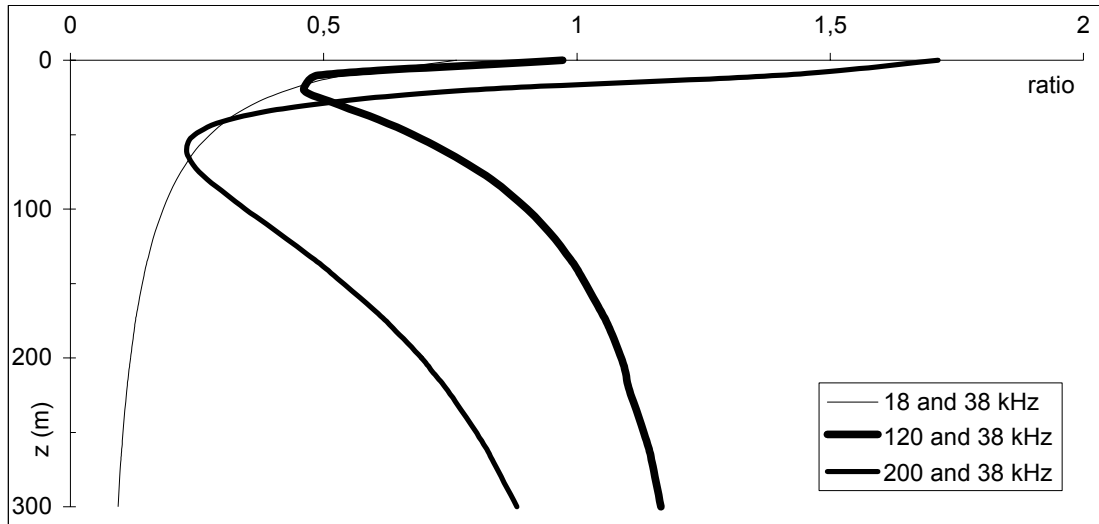


Fig. 3

Comparisons of the total backscattering cross sections at various frequencies.

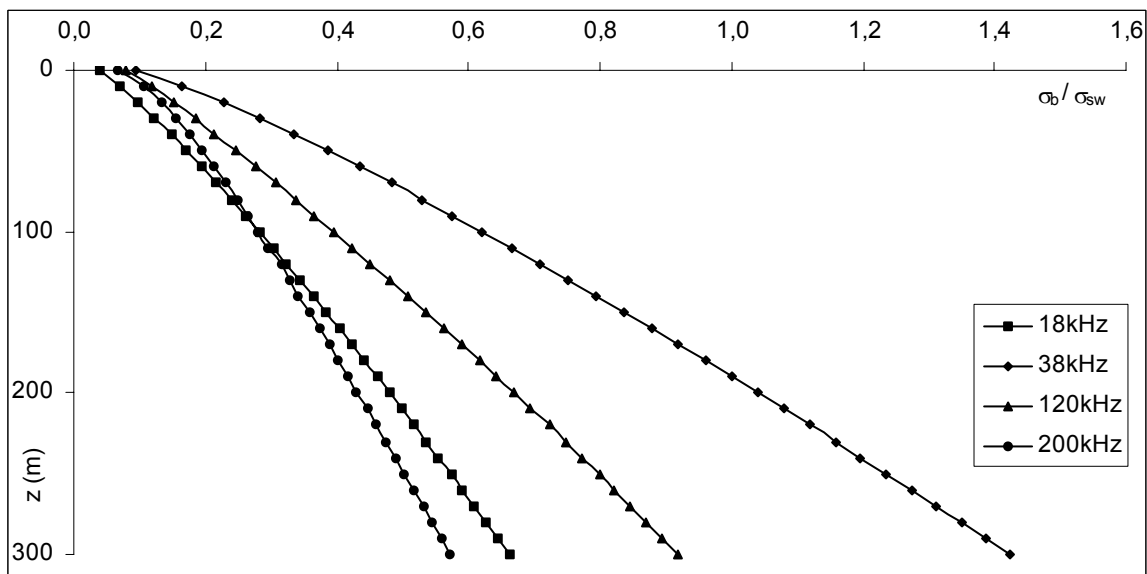


Fig. 4

Influence of fish flesh on the backscattering of the whole fish.

To understand how the fish body contributes into the backscattering of whole fish we computed the depth dependence of the ratio $\sigma_b/\sigma_{sw}(z)$ (where $\sigma_b = |f_b|^2$ is fish flesh backscattering cross section). The results are presented in Fig. 4. Various curves correspond to different frequencies – 18 (square-marked curve), 38 (diamonds), 120 (triangles) and 200 kHz (circles). The used computation parameters are the same as for Fig. 2. The calculations demonstrate that the fish flesh contribution increases with depth and also that it significantly depends on the frequency.

The significance of fish flesh contribution is also confirmed by the comparison of the results of the numerical analysis using the modified MB-DCM with the measurement data. The comparison is presented in Fig. 5, where the depth dependence of herring target strength at 38 kHz is presented. Here the circle-marked curve refers to the estimated model, which has been obtained fitting measurement data (maximum target strength data) by the non-linear regression (Ona *et al.* 2001b). The triangle-marked curve corresponds to the full free compression model (Ona *et al.*, 2001a). Diamond- and square-marked curves are obtained using the modified MB-DCM for the whole fish and swimbladder respectively.

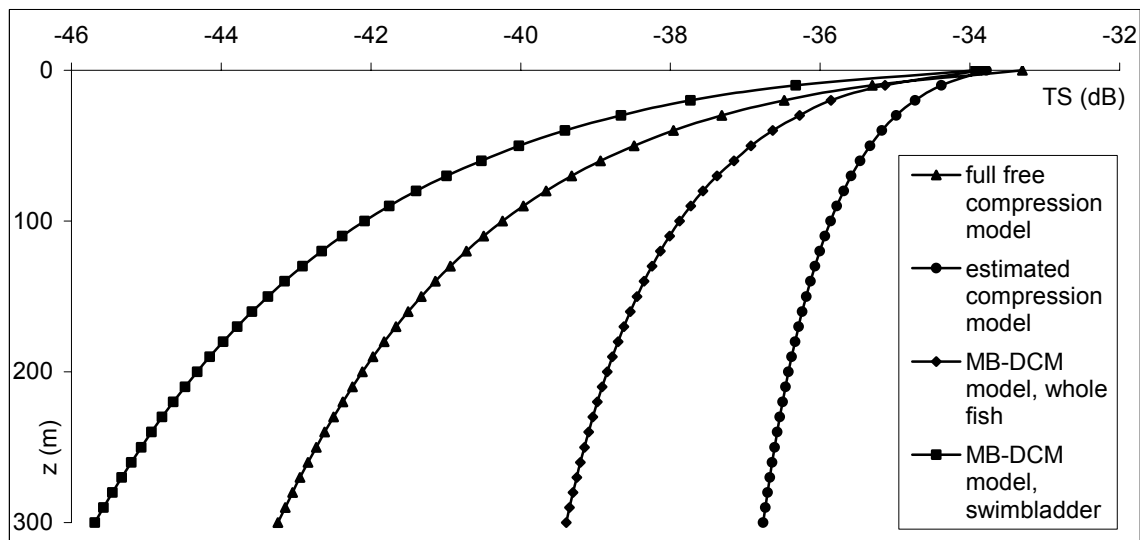
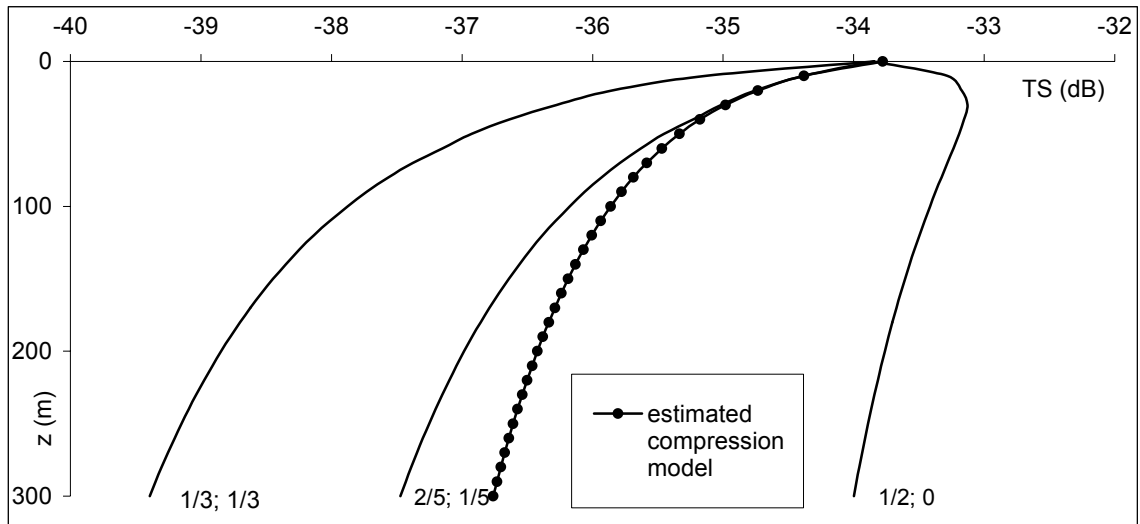


Fig. 5
Comparison with the measurement results at 38 kHz.

The computation parameters are the same as for Fig. 2. It is interesting to remark that the diamond-marked curve, which is obtained accounting the backscattering by both, by swimbladder and by fish body, is significantly closer to the measurement curve than the curve referring to swimbladder only (square-marked curve). This confirms that the fish flesh contribution is significant and should be considered in the explanation of the measurement depth dependent TS data.

As remarked above, the character of the deformation of each swimbladder dimension has yet not been studied in detail. It seems important to analyse the sensitivity of the backscattering with respect to the contraction factors α and β . The results of the numerical study of the whole fish target strength at the frequency 38 kHz are presented in Fig. 6. The marked curve in the plot is the result of fitting the measurement data (maximum target strength data) by the nonlinear regression method. (Ona *et al.* 2001b). The nonmarked curves refer to the computations made using the modified MB-DCM model. The two values presented near the each curves correspond respectively to the (α, β) values. The other

computed parameters are as in Fig 2. Choosing the (α, β) values, we take into account that the swimbladder backscattering cross section is grossly proportional to the dorsal geometrical cross section of the swimbladder. It is interesting to remark that the considered three cases differ in the rate of the depth variation of the dorsal geometrical cross section. The dorsal geometrical cross section area changes with depth as $\propto (1+z/10)^{-\eta}$, where $\eta = \alpha + \beta$. The contraction factor is the largest ($\eta = 2/3$) and the smallest ($\eta = 1/2$) for the cases $(\alpha=1/3, \beta=1/3)$ and $(\alpha=1/2, \beta=0)$ respectively. The case $(\alpha=2/5; \beta=1/5)$ is intermediate - the factor equals $3/5$.



*Fig. 6
Sensitivity of the depth dependence of the
whole fish target strength
to the contraction rates of individual dimensions of swimbladder at 38 kHz.
Comparison with the experimental results.*

The analysis of Fig. 6 demonstrates the sensitivity of whole fish backscattering cross sections to the character of the deformation of the individual swimbladder dimensions. The depth dependence of the backscattering cross section is steeper for larger contraction factor of the dorsal geometrical cross section deformation. In case $(\alpha=1/3, \beta=1/3)$, where the contraction factor is the largest, the dependence is steepest. It demonstrates that the knowledge of the swimbladder dimension contraction rates is important to interpret the measurement data.

It also interesting to note that the marked curve, obtained on the basis of the measurements, lies between the curves corresponding to the $\eta = 2/5$ and $\eta = 1/2$, which allow to suppose that the contraction rate of swimbladder dorsal cross section area belong to this range.

CONCLUSIONS

The analysis, based on the MB-DCM model, in which the depth dependent contraction of fish swimbladder and backscattering by the fish flesh have been introduced, and the comparison with the measurement data allow to conclude:

1. The depth dependence of herring target strength is significant at the frequencies used in herring abundance estimation. The frequency dependence of herring target strength also varies with depth.
2. The fish flesh can significantly influence the backscattering by the whole fish. The contribution is depth- and frequency-dependent.
3. The herring target strength is sensitive to the contraction rate of the individual swimbladder dimensions or to the reduction rate of swimbladder dorsal cross section area. The rates define the reduction rate of the whole fish target strength with depth.
4. The reasonable fit between the measurement data and the results obtained on the basis of the modified MB-DCM, accounting for the swimbladder depth contraction and the fish flesh influence, has been demonstrated.
5. Further theoretical analysis taking into account the complicated morphology of herring swimbladder is reasonable. Studies of how the individual swimbladder dimensions reduces with depth – is important.

REFERENCES

- Blaxter, J.H.S. 1979. The herring swimbladder as a gas reservoir for the acoustico - lateralis system. *Journal of the Marine Biological Association of the United Kingdom*, 59: 1–10.
- Blaxter, J.H.S., and Batty, R.S. 1984. The herring swimbladder: loss and gain of gas. *Journal of the Marine Biological Association of the United Kingdom*, 64: 441–459.
- Brawn, V.M. 1962. Physiological properties and hydrostatic function of the swimbladder of herring (*Clupea harengus*). *Journal of the Fisheries Research Board of Canada*, 19: 635–655.
- Fahlen, G. 1967. Morphological aspects of the hydroacoustic function of the gas bladder in *Clupea harengus*. *Acta Universitatis Lundensis (University of Lund), Sweden.*, 49: no. 1.
- Furusawa, M. 1988. Prolate spheroidal models for predicting general trends of fish target strength. *Journal of the Acoustical Society of Japan (E)*, 9: 13 – 24.
- Medwin, H., and Clay, C.S. 1998. *Fundamentals of Acoustical Oceanography*. Ed. by R. Stern and M. Levy. Academic Press, San Diego. 712pp.
- Ona, E. 1990. Physiological factors causing natural variations in acoustic target strength of fish. *Journal of the Marine Biological Association of the United Kingdom*, 70: 107–127.
- Ona, E., Svellingen, I., and Fosseidengen, J.E. 2001a. Target strength of herring during vertical excursions. ICES Fisheries Acoustics, Science and Technology Working Group (FAST), Seattle, April 2001, 1-16
- Ona, E. , Vabø, R., Huse, I. and Svellingen I. 2001b. Depth dependent target strength in herring. (Submitted to *ICES Journal of Marine Science*).
- Stanton, T. K. 1988. Sound scattering by cylinder of finite length. I. Fluid cylinders. *Journal of the Acoustical Society of America*, 83: 55 – 63.
- Stanton, T. K. 1989. Sound scattering by cylinder of finite length. III. Deformed cylinders. *Journal of the Acoustical Society of America*, 86: 691 – 705.

Ye, Z., and Farmer, D. 1996. Acoustic scattering by fish in the forward direction. ICES Journal of Marine Science, 53: 249 – 252.

Ye, Z., and Furusawa, M. 1995. Modelling of target strength of swimbladder fish at high frequencies. Journal of the Acoustical Society of Japan, (E), 16: 371–379.

Ye, Z. 1996. On acoustic attenuation by swimbladder fish. Journal of the Acoustical Society of America, 100: 669-672.